A Molecular Link between Cell Wall Modification and Stringent Response in a Gram-positive Bacteria

Running Title: Cell wall modification protein regulates stringent response pathway

Surya D. Aggarwal[1], Saigopalakrishna S. Yerneni[2], Ana Rita Narciso[3,4], Sergio R. Filipe[3,4], N. Luisa Hiller[1]*

[1]Dept. of Biological Sciences, Carnegie Mellon University, Pittsburgh, PA, USA
[2]Dept. of Biomedical Engineering, Carnegie Mellon University, Pittsburgh, PA, USA
[3]Laboratory of Bacterial Cell Surfaces and Pathogenesis, Instituto de Tecnologia Química e Biológica António Xavier, Universidade Nova de Lisboa, Oeiras, Portugal
[4]UCIBIO-REQUIMTE, Departamento de Ciências da Vida, Faculdade de Ciências e Tecnologia, Caparica, Portugal

*corresponding author: lhiller@andrew.cmu.edu

Keywords: Gram-positive, *Streptococcus pneumoniae*, cell wall, translation quality control, stringent response, alarmone, autolysis, phagocytosis

ABSTRACT

To ensure survival during colonization of the human host, bacteria must successfully respond to unfavorable and fluctuating conditions. This study explores the fundamental phenomenon of stress response in a gram-positive bacterium, where we investigate the ability of a cell wall modification enzyme to modulate intracellular stress and prevent the triggering of the stringent response pathway. The *Streptococcus pneumoniae* cell wall modification proteins MurM and MurN are tRNA-dependent amino acid ligases, which lead to the production of branched muropeptides by generating peptide crossbridges. In addition, MurM has been proposed to contribute to translation quality control by preferentially deacylating mischarged tRNAs mischarged with amino acids that make up the peptidoglycan. Here, we demonstrate that the *murMN* operon promotes optimal growth under stressed conditions. Specifically, when grown in mildly acidic conditions, a *murMN* deletion mutant displays early entry into stationary phase and dramatically increased lysis. Surprisingly, these defects are rescued by inhibition of the stringent response pathway or by enhancement of the cell's ability to deacylate mischarged tRNA molecules. The increase in lysis results from the activity of LytA, and experiments in macrophages reveal that *murMN* regulates phagocytosis in a LytA-dependent manner. These results suggest that under certain stresses, these bacterial cells lacking MurMN likely accumulate mischarged tRNA molecules, activate the stringent response pathway, and enter prematurely into stationary phase. Moreover, by virtue of its ability to deacylate mischarged tRNAs while building peptidoglycan crossbridges, MurM can calibrate the stress response with consequences to host-pathogen interactions. Thus, MurM is positioned at the interface of cell wall modification, translation quality control and stringent response. These findings expand our understanding of the functions of the bacterial cell wall: cell wall modifications that impart structural rigidity to the cell are interlinked to the cell's ability to signal intracellularly and mount a response to environmental stresses.

SIGNIFICANCE

During infection, microbes must survive the hostile environmental conditions of the human host. When exposed to stresses, bacteria activate an intracellular response, known as stringent response pathway, to ensure their survival. This study connects two fundamental pathways important for cellular growth in a gram-positive bacterium; it demonstrates that enzymes responsible for cell wall modification are connected to the stringent response pathway via their ability to ameliorate errors in protein translation. Our study was performed on *Streptococcus pneumoniae* where the cell wall modification enzyme, MurM, is a known determinant of penicillin resistance. We now demonstrate the importance of MurM in translation quality control and establish that it serves as a gatekeeper of the stringent response pathway.

INTRODUCTION

Gram-positive bacteria have evolved a thick and sophisticated cell wall that ensures bacterial structural integrity and is critical for cellular viability. This dynamic structure serves as a scaffold for surface anchored proteins, wall teichoic acids, lipoteichoic acids, lipoproteins, and capsular polysaccharides (1, 2). It is also a major target of immune defenses and antibiotics (3, 4). Opportunistic pathogens, such as *Streptococcus pneumoniae* (pneumococcus), encounter hostile environments within the human host, where the cell wall serves as a barrier and an interface between the bacteria and its host.

The pneumococcal cell wall consists of glycan chains that are cross-linked via peptide bridges (5). These glycan chains consist of alternating subunits of *N*-acetylglucosamine (NAG) and *N*-acetylmuramic acid (NAM) residues. Each NAM subunit is attached to a peptide side chain, which is crosslinked to stem peptide from another glycan chain. In pneumococcus, the link can be direct or through a short diamino acid peptide bridge that is assembled by MurM and MurN, two tRNA-dependent amino acid ligases. These proteins add the diamino acid peptide to the lipid II peptidoglycan precursor in the inner side of the bacterial membrane before this complex is flipped to the outer side, where the peptidoglycan building block containing this diamino acid peptide is incorporated into the cell wall by penicillin binding proteins (6). The peptide bridge originates from the third residue (L-Lys) on one pentapeptide chain and is ultimately connected to the fourth residue (D-Ala) of the stem peptide in a neighboring glycan chain (6, 7). MurM contributes either an alanine or a serine to the first position of the bridge, while MurN contributes an alanine to the second position. Thus the pneumococcal peptidoglycan peptide bridge consists of either L-Ala-L-Ala or L-Ser-L-Ala. Allelic variants of *murM* alone lead to diversity in the nature of stem peptide branching in the cell wall peptidoglycan (8–10). Finally, *murMN* are

86 required for penicillin resistance, as inactivation of this operon leads to a complete loss of
87 penicillin resistance (6, 11).
88
89 As tRNA-dependent amino acid ligases, MurMN acquire the alanines and serines they utilize for
90 the peptidoglycan bridge from aminoacyl-tRNAs. The employment of charged tRNAs as
91 substrates for MurMN is an evolutionary design that juxtaposes the fundamental cellular
92 functions of peptidoglycan biosynthesis and protein translation. Previous work has
93 demonstrated that MurM can deacylate mischarged tRNAs (12). Moreover, *in vitro*, it displays a
94 substantial preference for deacylating mischarged tRNAs over correctly charged tRNAs (13).
95 The preference for amino acids from mischarged tRNAs strongly suggests that MurM decreases
96 the pool of mischarged tRNAs present in the cell, thereby, contributing to the process of
97 translation quality control (12).
98
99 Under stress, many bacterial cellular processes including translation, are regulated by the
100 stringent response pathway. Deprivation of amino acids or carbon sources, elevated
101 temperature, and acidic conditions can trigger the stringent response and rewire the cellular
102 circuitry to adapt to challenging conditions and ensure bacterial survival (14–17). In addition, the
103 stringent response plays a role in regulation of bacterial virulence and susceptibility to
104 antimicrobials (15, 18–20). The stringent response pathway is characterized by the
105 accumulation of alarmones, specifically guanosine tetra- (ppGpp) and pentaphosphate
106 (pppGpp). In the majority of gram-negative bacteria, these are produced by RelA. In gram-
107 positive bacteria, these are produced by a bifunctional RSH protein (RelA/SpoT homolog), with
108 both synthetase and hydrolase activity (16, 21). In gram-negative bacteria, binding of
109 deacylated-tRNA to ribosomes activates alarmone production (22–25), however, the molecular

mechanisms underlying activation of the stringent response pathway in gram-positive bacteria remain elusive.

In this study, we show that MurMN is a molecular link between the processes of cell wall modification and translation quality control. Our findings indicate that the absence of these proteins sensitizes pneumococcal cells to acidic stress: when a *murMN* deletion mutant strain is grown in mildly acidic conditions, growth defects result from the likely accumulation of mischarged tRNAs and the activation of the stringent response pathway. Further, our data suggest that activation of the stringent response stimulates LytA activity and subsequently influences pneumococcal cells' ability to be phagocytosed. These findings provide insight into cell wall function by suggesting that the cell wall modification enzymes can buffer intracellular stress and modulate activation of the stringent response pathway.

RESULTS

The *murMN* operon protects cells against acid-induced growth defects

When growing a *ΔmurMN* strain in planktonic culture, we observed a pronounced growth defect in rich media in mildly acidic conditions (pH 6.6) **(Fig. 1A)**. The mutant exhibited increased susceptibility to stationary-phase induced autolysis and a decrease in the maximum optical density reached after growth (max OD), consistent with an early onset of stationary phase. This growth defect was rescued in a *ΔmurMN* complemented strain (*ΔmurMN*:*murMN*) **(Fig. 1B and 1C)**. Although minor differences in growth of wild-type and *ΔmurMN* strains were observed in rich media at normal conditions (pH 7.4), these differences were much more pronounced in mildly acidic conditions.

MurMN contribute to cell wall branching by adding diamino acid peptide bridges to the peptidoglycan stem peptide that lead to production of branched muropeptides (6). The loss of branching alters pneumococcal cell wall composition and increases bacterial sensitivity to lysis by cell wall inhibitors (26). Thus, one hypothesis for the difference in sensitivity of wild-type and *ΔmurMN* strains to acidic stress is that wild-type cells incur changes in the cell wall in response to pH, and that these chances are absent in a *ΔmurMN* strain. To test this hypothesis, we employed high-performance liquid chromatography (HPLC) to analyze the peptidoglycan composition of pneumococci grown in rich media at normal (pH 7.4) and mildly acidic (pH 6.6) conditions for both wild-type and *ΔmurMN* strains. We did not observe any differences in the cell wall composition of the wild-type cells between normal and acidic conditions **(Fig. 2Ai, B)**. Similarly, there was also no difference in the cell wall composition of *ΔmurMN* cells between normal and acidic conditions **(Fig. 2Aii, B)**. As expected, we observed that deletion of *murMN* led to the loss of branched peptides from the peptidoglycan compared to wild-type cells. These findings suggest that the growth differences observed in the *ΔmurMN* strain in acidic conditions cannot be attributed to pH-dependent alterations in peptidoglycan composition.

Disruption of the translation quality control function of MurM leads to pneumococcal growth defects

Recent *in vitro* experiments have shown that MurM can deacylate mischarged tRNAs, and that it may play a significant role in maintaining low levels of mischarged tRNAs in pneumococcal cells (12). Given that the growth defect of the *ΔmurMN* strain could not be attributed to alterations in the cell wall composition in acidic conditions **(Fig. 2)**, we hypothesized that the loss of the translation quality control role of MurM was responsible for the observed phenotypes.

In addition to obtaining alanine or serine from correctly aminoacylated-tRNAs (Ala-tRNA^{Ala} or Ser-tRNA^{Ser} respectively), MurM can also acquire these amino acids from other mischarged tRNA species (12, 27). In fact, alanyl-tRNA synthetase (AlaRS), the enzyme responsible for charging tRNA^{Ala} to produce Ala-tRNA^{Ala} is error prone, such that tRNA^{Ala} is often misactivated with serine (Ser-tRNA^{Ala}) or glycine (Gly-tRNA^{Ala}) (28) **(Fig. 3B)**. Accumulation of Ser-tRNA^{Ala} is toxic to cells such that many organisms, across all the three kingdoms of life, encode a free-standing homolog to the editing domain of AlaRS protein, termed AlaXp. These AlaXp prevent toxicity by deacylating mischarged tRNA^{Ala} molecules in different organisms (29–33). Interestingly, analysis of the *S. pneumoniae* available genomes, suggests that pneumococcus does not encode an AlaXp protein; instead, once the tRNA molecules are charged, the responsibility of ensuring translational fidelity has been proposed to rest with MurM by virtue of its deacylation function (12, 34). Importantly, the catalytic efficiency of MurM in using mischarged Ser-tRNA^{Ala} as a substrate for generating crosslinks is dramatically higher relative than its ability to use correctly acylated Ala-tRNA^{Ala} or Ser-tRNA^{Ser} (13). The high affinity of MurM for misacylated-tRNA^{Ala} combined with the absence of a gene encoding AlaXp in the pneumococcal genome, emphasize the importance of MurM in translation quality control.

We reasoned that expression of a tRNA-editing protein in a *ΔmurMN* background could allow us to distinguish between the cell-wall crosslinking and the translation quality control roles of MurM, and thus establish which of these roles is responsible for the growth defect of the *ΔmurMN* strain. To this end, we overexpressed the editing domain of AlaRS protein. We determined the editing domain of the protein encoded by pneumococcal *alaRS* (*spr_1240*) using an amino acid alignment with AlaRS proteins from *E. coli* (WP_096112793.1) and *B. subtilis*

(WP_007408211.1), where the protein domains have been well characterized (30, 31, 35). The pneumococcal editing domain was identified as residues 437-873 of the pneumococcal AlaRS, and the peptide encoded by this region was used for functional complementation ($AlaRS_{editing}$) **(Fig. 3A)**. Ectopic expression of $AlaRS_{editing}$ is predicted to deacylate mischarged alanine-specific tRNA species ($tRNA^{Ala}$), the most abundant of which are Ser-$tRNA^{Ala}$ and Gly-$tRNA^{Ala}$ (12, 28) **(**blue in **Fig. 3B)**. Since $AlaRS_{editing}$ only deacylates mischarged $tRNA^{Ala}$ molecules, its expression will not diminish the correction of other mischarged tRNA species ($tRNA^{Ser}$, $tRNA^{Phe}$, $tRNA^{Lys}$), which are also thought to be employed by MurM to acquire non-cognate alanine or serine (12, 13, 27) **(**green in **Fig. 3B)**.

The expression of $AlaRS_{editing}$ in the *ΔmurMN* strain partially rescued the growth defect displayed by the *ΔmurMN* strain in mildly acidic conditions **(Fig. 3C)**. Specifically, the *ΔmurMN::alaRS*$_{editing}$ strain resembled the wild type in that it did not exhibit the dramatically increased stationary-phase induced lysis associated with the *ΔmurMN* and its maxOD was intermediate between the *ΔmurMN* and wild-type strains. These finding illustrate the importance of the deacylating function of MurM *in vivo* and imply that MurM ensures normal growth in mildly acidic conditions by its ability to deacylate mischarged tRNAs, which would be toxic for pneumococcal cells.

MurMN regulate activation of the stringent response pathway

The stringent response is a well conserved pathway utilized by bacteria to ensure survival under stressed conditions. Mediated by the production of alarmones, the activation of this pathway rewires the cellular circuitry and coordinates cellular entry into stationary phase (36). We

206 hypothesized that the differences in growth of the *ΔmurMN* strain, relative to the wild-type strain,
207 are a consequence of activation of the stringent response pathway.
208
209 If activation of the stringent response pathway contributes to the early onset of stationary phase
210 in the *ΔmurMN* strain, this growth phenotype should be decreased or abrogated in a *ΔmurMN*
211 where the stringent response pathway cannot be activated. This pathway is activated by
212 accumulation of the intracellular alarmones, ppGpp or pppGpp, which are hyperphosphorylated
213 forms of GDP or GTP respectively, synthesized by the addition of a pyrophosphate molecule
214 obtained from ATP **(Fig. 4A)**. In pneumococcus, the primary source of alarmone production is
215 RSH (RelA/SpoT Homolog), a bifunctional synthetase and hydrolase of (p)ppGpp (37). Thus,
216 we deleted *rsh* (*spr_1487*) to generate strains defective in the ability to activate the stringent
217 response pathway. Thin-layer chromatography experiments were used to confirm that the *Δrsh*
218 strain did not produce measurable levels of alarmone **(Fig. 4B)**.
219
220 We compared growth among wild-type, *ΔmurMN,* and*ΔmurMNΔrsh* strains **(Fig. 4C)**.
221 The *ΔmurMNΔrsh* strain did not exhibit the growth defects observed for the *ΔmurMN* strain in
222 mildly acidic conditions. Thus, inhibition of the stringent response abrogates the growth defects
223 in a *ΔmurMN* background. To measure the relative alarmone levels in the *ΔmurMN* strain
224 relative to the wild-type strain in mildly acidic conditions, we employed thin-layer
225 chromatography (TLC). The *ΔmurMN* strain displays increased alarmone levels compared to the
226 wild-type strain, as observed by the higher levels of alarmone relative to GTP, consistent with
227 growth defects in the absence of *murMN* **(Fig. 4B)**. We conclude that acidic conditions promote

entry into stringent response, and that MurMN buffer the activation of stringent response and consequently entry into stationary phase.

It is well established that *murMN* is required for penicillin resistance of pneumococci (6). We investigated whether the fitness of *ΔmurMN* strain under penicillin pressure can be enhanced by inhibition of the stringent response pathway. To this end, we determined the percentage of viable pneumococcal cells when grown at a concentration of penicillin, that is approximately equal to the minimum inhibitory concentration of this antibiotic for the *ΔmurMN* strain (0.025 µg/ml). At this concentration, the *ΔmurMNΔrsh* and the *ΔmurMN::alaRS*$_{\text{editing}}$ strains displayed a marked increase in survival relative to the *ΔmurMN* background (**Table 1**). We conclude that the role of MurM in preventing the activation of the stringent response, due to correction of mischarged tRNAs, contributes to increase in fitness under penicillin pressure.

murMN dampen LytA-mediated lysis

The early onset of stationary phase is followed by increased lysis in the *ΔmurMN* strain when grown in mildly acidic conditions **(Fig. 1)**. Having established that *murMN* regulate activation of the stringent response pathway, we searched for the molecule(s) responsible for the autolysis. Autolysis of pneumococcal cells is carried out by autolysins, peptidoglycan hydrolases containing choline-binding domains that enable their binding to phosphocholine residues present on the teichoic acids of the cell wall (38–40). Lysis requires attachment of choline-binding proteins to the cell surface, such that addition of exogenous choline inhibits this binding and the consequent autolysis (38, 41–43). Addition of two percent choline chloride to *ΔmurMN* grown in mildly acidic conditions abrogated lysis, suggesting lysis is triggered by choline binding

protein(s) **(Fig. 5A)**. Of the multiple choline binding proteins encoded in the pneumococcal genomes, LytA is the major autolysin. To investigate whether the increased lysis of *ΔmurMN* is induced by LytA, we tested growth of *ΔmurMN* with a deletion in *lytA* (*ΔmurMNΔlytA*). The *ΔmurMNΔlytA* strain resembled the wild-type strain in that it did not display lysis **(Fig. 5B)**. Further, the lower maxOD observed in *ΔmurMN* strain was not rescued to wild type levels in the *ΔmurMNΔlytA* strain **(Fig. 5B)**. This rescue of only the lysis phenotype in the *ΔmurMNΔlytA* strain suggests that in the absence of *murMN*, activation of the stringent response induces early onset of stationary phase and that LytA is responsible for the subsequent autolysis phenotype. The dramatically increased sensitivity of the *ΔmurMN* to LytA activity, relative to both the wild-type strain at mildly acidic and the *ΔmurMN* strain at normal conditions, suggest that *murMN* suppress the activation of LytA under mildly acidic conditions **(Fig. 5C)**.

MurMN influence macrophage phagocytosis by regulating LytA activity

Pneumococcal cells encounter numerous environmental stresses in an infection setting. Among these is acidic pH, encountered as a result of the inflammatory response mounted by the host against the invading bacteria (44, 45). Moreover, previous work suggests that LytA contributes to pneumococcal evasion from phagocytosis (46), and our data revealed that the *ΔmurMN* strain displays increased LytA mediated autolysis. Thus, we hypothesized that macrophages would be less efficient at uptaking the *ΔmurMN* strain relative to wild-type cells.

To test for phagocytosis, we moved to the encapsulated strain D39, the serotype 2 strain which is the ancestor of R6D. Macrophages were tested for their ability to phagocytose D39 and its isogenic mutants. In support of our hypothesis, the number of macrophages positive for

pneumococcus was lower when infected with *ΔmurMN* strain relative to the wild-type strain **(Fig. 6, S1)**. Further, this phenotype was reversed for the *ΔmurMNΔlytA* strain, demonstrating the importance of LytA in this phenotype **(Fig. 6, S1)**. Finally, in agreement with previous work (46), the number of macrophages positive for pneumococcus was increased upon infection with a *ΔlytA* strain **(Fig. 6, S1)**.

Our data suggest that the activation of LytA in the *ΔmurMN* strain requires activation of the stringent response pathway. In support, the number of macrophages that internalize the *ΔmurMNΔrsh* strain was higher than those that internalize the *ΔmurMN* strain. Finally, our model predicts that *murMN* buffers the stringent response and LytA activation via its role in deacylating the misacylated tRNAs. Consistently, we observed a higher number of macrophages positive for the *ΔmurMN::alaRS*$_{editing}$ strain relative to the *ΔmurMN* strain **(Fig. 6, S1)**. These data are consistent with a role for *murMN* in activation of the stringent response and consequent increase in LytA activity and capture the consequence of *murMN*-mediated stringent response suppression for phagocytosis.

The decreased percentage of macrophages positive for the *ΔmurMN* strain could be a consequence of either greater evasion of pneumococcal cells from phagocytosis or increased lysis of pneumococcal cells upon their internalization. If the acidic environment of macrophages promotes increased lysis of the *ΔmurMN* strain, there should be a rapid decrease in internalized bacteria over time. In contrast, we observe a more gradual decline in internalized *ΔmurMN* relative to the wild-type strain **(Fig. S2)**. Thus, the *ΔmurMN* strain appears to evade phagocytosis, and, as previously reported, this process is LytA-dependent (46).

DISCUSSION

Elucidating the mechanisms that bacterial cells employ to compartmentalize their functions or organize cell-wide responses to environmental stresses is fundamental to the field of microbiology. The tRNA-dependent-amino acid ligases involved in cell wall modification are optimally positioned to play a dual role in the cell: they build peptide crossbridges that serve as a major component of the bacterial cell wall, and they deacylate mischarged tRNAs, carrying out a vital role of translation quality control. Some bacterial species have evolved mechanisms to divert aminoacylated tRNA molecules away from translation and toward cell wall biosynthesis (12). For instance, *Staphylococcus aureus* encodes a set of isoacceptor tRNA species that display a greater propensity for peptidoglycan biosynthesis then translation, via diminished binding to the EF-Tu elongation factor utilized in translation (47). Similarly, *Mycobacterium tuberculosis* encodes dedicated tRNA synthetases that are spatially tethered to cell wall biosynthesis enzymes, and thus are exclusively used in the peptidoglycan (48). In contrast, in other bacterial species, the same pool of aminoacyl tRNAs serves both peptidoglycan modification and translation (49). Our data suggest that in this organization, cell wall tRNA-dependent-amino acid ligases can serve as regulators of intracellular stress. Our studies in the pneumococcus reveal that diminished editing and likely accumulation of mischarged tRNAs initiates the stringent response, premature entry into stationary phase, and subsequent activation of the murein hydrolase LytA. In this context, the cell wall modification protein MurM, by virtue of its role in deacylating mischarged tRNAs, dampens activation of the stringent response and calibrates the cellular reaction to stress.

An outstanding question in this model is how do mischarged tRNAs trigger the stringent response? Binding of aminoacyl tRNA to the ribosomal A-site provides the required amino acid

for polypeptide elongation (16). In gram-negative bacteria, binding of deacylated tRNAs to the ribosome activates RelA and induces alarmone production (16). Activation of the stringent response is less understood in gram-positive bacteria, where the alarmone synthetase and hydrolase functions are fused in the bifunctional RSH enzyme (14, 50, 51). We propose that the accumulation of misacylated tRNAs, due to the absence of functional MurMN proteins, may also trigger the stringent response. Classic translation models suggest that the translation machinery recognizes the EF-Tu bound aminoacylated tRNA without displaying specificity for the amino acid, such that some amino acids from mischarged tRNAs can be incorporated into protein (52–55). However, other evidence suggest that the translation machinery recognizes both the amino acid and the tRNA: strong binding affinities of EF-Tu to tRNAs are compensated by weak binding affinities of EF-Tu to amino acids and vice-versa, leading to uniform binding affinities across tRNAs charged with their cognate amino acid (56). In this case, misacylated tRNAs can display binding affinities to the EF-Tu that are dramatically different than correctly charged tRNAs (57). Given the considerable difference in the inherent EF-Tu binding affinities of $tRNA^{Ala}$ and $tRNA^{Ser}$ (56, 58–60), it is expected that incorporation of $Ser\text{-}tRNA^{Ala}$ will lead to an appreciable change in translation efficiency. Combined with our result that accumulation of mischarged tRNAs trigger the stringent response in pneumococcus, it seems plausible that RSH may be activated by binding of mischarged tRNAs to the ribosome.

Previous work has characterized the only RSH present in the pneumococcus, and established its important in alarmone production (37). The pneumococcal RSH contributes to copper uptake, provides increased fitness in cells subjected to mupirocin (an antibiotic that causes amino acid (Ile) starvation), and is a virulence determinant in the murine models of pneumococcal pneumoniae and sepsis (37). Further, studies of a RSH point mutation identified in a laboratory

345 variant of a clinical strain, demonstrated that RSH promotes resistance to neutrophil killing and
346 provides a fitness advantage in a murine model of colonization (61). Together, these studies
347 strongly suggest that the ability of pneumococcus to trigger the stringent response is critical for
348 virulence. We put forward the idea that MurMN play a role in fine-tuning entry into the stringent
349 response, and as such may contribute to the outcome of pneumococcal infections. This could
350 explain why most bacteria carry the *murMN* operon despite lacking a peptidoglycan rich in the
351 branched muropeptides that are the product of the MurMN proteins.
352
353 Our work describing a novel role for *murMN* was performed using growth in a mildly acid
354 condition. Bacterial cells commonly encounter acidic environment in the human host during
355 infection due to inflammation response mounted by immune cells (45). There are a series of
356 studies on molecular responses of pneumococcal cells subjected to acid stress (62–65). These
357 studies describe the molecular regulation of acidic stress-induced lysis, a response mediated by
358 LytA and regulated by phosphorylation of ComE in a competence stimulating peptide-
359 independent manner (63–65). These studies differs from our work in design and scope. First,
360 while we also focus on pneumococcal growth in acidic pH, these studies analyzed cells pre-
361 conditioned in alkaline pH before exposure to acidic stress. Second, our work is centered on
362 *murMN* and its role in the cellular response to acidic stress. The growth defect we describe is
363 not observed in a *ΔcomE* strain and the growth of the *ΔmurMNΔcomE* strain resembles that of
364 *ΔmurMN* strain (data not shown). Thus, the molecular responses described in this study do not
365 appear to overlap with those previously described and highlights the importance of *murMN* in
366 regulation of growth in mildly acidic conditions.
367

368 The *ΔmurMN* strain is prone to LytA-mediated lysis, and this effect is dramatic at a mildly acid
369 pH. The dynamics of LytA during planktonic growth have been well characterized (66). During
370 exponential growth, LytA is mainly intracellularly and inactive. During stationary phase, LytA
371 exits the cells, where it promotes autolysis via its *N*-acetylmuramoyl-L-alanine amidase activity
372 and in doing so breaks the amidase bond between the carbohydrate and the peptide
373 components of the peptidoglycan backbone (67). Thus, the activation of LytA in the *ΔmurMN*
374 strain can be explained by its early onset into stationary phase. In addition, previous work has
375 demonstrated that LytA contributes to evasion from phagocytosis by inhibition of complement-
376 mediated immunity (46). LytA inhibits binding of proteins in the classical complement pathway to
377 the pneumococcal surface and enhances recruitment of suppressors of complement to impair
378 the alternative complement pathway. Thus, we hypothesized that increased activity of LytA in
379 the *ΔmurMN* strain would protect it from macrophage uptake. As predicted, the number of
380 macrophages with internalized pneumococci was lower for the *ΔmurMN* relative to the wild-type
381 strain. Moreover, this phenotype was reversed in a *ΔmurMNΔlytA* mutant. These data are
382 consistent with our conclusion that *murMN* restrains LytA activity. Further, our experiments in
383 macrophages combined with previous work on *Δrsh* strains (37, 61) suggest that pneumococcal
384 fitness *in vivo* may depend on careful calibration of the stringent response, where activation and
385 timing can expose or conceal pneumococcus to different facets of the immune response.
386
387 MurM is encoded in all pneumococcal strains as well as some related species, and there are
388 multiple *murM* alleles (9, 68–70). All pneumococcal *murM* alleles have the ability to introduce
389 both serine and alanine at the first position of the diamino acid peptide bridge (8). However,
390 alleles vary regarding expression levels and the relative ratio of serine versus alanine they insert

391 in the first position of the peptide bridge (8, 26). Thus, *murM* alleles may also vary in their ability
392 to deacylate mischarged Ser-tRNA^{Ala} and control entry into the stringent response.
393
394 In nature, there is one free standing editing protein, AlaXp, and it deacylates Ser-tRNA^{Ala} and
395 Gly-tRNA^{Ala}. AlaXp is homologous to the editing domain of the AlaRS alanyl-tRNA synthetase
396 protein, which possesses both synthetase and editing functions (33). The conserved
397 widespread distribution of AlaXp across the tree of life contrasts with the limited phylogenetic
398 distribution of other standalone aminoacyl-tRNA editing proteins and highlights the importance
399 of the AlaXp function. Further, analysis of characterized AlaXp proteins reveals that they are
400 conserved in their ability to deacylate Ser-tRNA^{Ala} , but not necessarily Gly-tRNA^{Ala} molecules
401 (33). These findings suggest that deacylating mischarged Ser-tRNA^{Ala} is of great importance to
402 the cell, and that accumulation of this mischarged tRNA is toxic to the cell. Thus, it has been
403 proposed that AlaXp is an evolutionary solution to the ubiquitous challenge of Ser-tRNA^{Ala}
404 production. The overlap in function between MurM and AlaXp suggests that MurM may also
405 represent an alternative evolutionary solution to the challenge of editing Ser-tRNA^{Ala} (34). Our
406 genomic search reveals that many Firmicutes that produce peptide bridges, such as
407 *Staphylococcus aureus*, *Streptococcus thermophilus*, *Streptococcus agalactiae*, *Streptococcus*
408 *salivarius, Enterococcus faecalis* and *Lactobacillus viridescens*, do not appear to encode for an
409 AlaXp protein. It is thus tempting to speculate that the composition of cell wall bridges, the vast
410 majority of which utilize serine, alanine, or glycine, may represent an adaptation that reflects the
411 function of cell wall tRNA synthetases in translation quality control.
412
413 In conclusion, this study suggests that MurM provides a molecular link between cell wall
414 modification and translation quality control in gram-positive bacteria that produce short peptide
415 bridges in their peptidoglycan layer. These bridges are structural components with a critical role

in antibiotic resistance (6–8, 11). This study provides *in vivo* evidence to suggest that the propensity of MurM to deacylate mischarged-tRNA allows it to serve as a translation quality control checkpoint and dampen entry into the stringent response. Through these mechanisms, MurM regulates the activity of LytA and influences phagocytosis. These findings implicate MurM in the survival of bacteria as they encounter unpredictable and hostile conditions in the host. The question of how the regulation of these fundamental biological processes by MurM influences the extent of pathogenesis still remains to be investigated. Our work provides functional insight into the role of peptidoglycan peptide bridge generating enzymes in modulating intracellular stress and entry into the stringent response.

MATERIALS & METHODS

Bacterial strains & growth conditions

This experimental work was performed on two strains of *Streptococcus pneumoniae* and their isogenic mutants. The majority of the work was performed on a penicillin-resistant derivative of R6 (R6D). This R6D isolate, also referred to as Hun663.tr4, was generated from a genetic cross where parental R6 strain was recombined with DNA isolated from Hungary19A-6 and recombinants were selected for penicillin resistance (71). The *murM* allele in this strain correspond to allele *murMB1*. R6D is a non-encapsulated strain, thus the macrophage experiments were performed with the highly related serotype 2 D39 strain (*murMA* allele) and isogenic mutants (GenBank CP000410) (72).

Colonies were grown from frozen stocks by streaking on TSA-II agar plates supplemented with 5% sheep blood (BD BBL, New Jersey, USA). Colonies were then picked and inoculated in fresh Columbia broth (Remel Microbiology Products, Thermo Fisher Scientific, USA) and incubated at 37°C and 5% CO_2 without shaking. For acidic conditions, the pH of the Columbia

441 broth was adjusted to 6.6 by the addition of 1M HCl. The basic recipe used for preparing
442 chemically defined medium (CDM) was as previously described (73). MOPS-CDM was
443 prepared by replacing potassium phosphate and sodium phosphate as previously described
444 (37).
445
446 **Construction of mutants**
447 The deletion mutant strains were constructed by using site-directed homologous recombination
448 to replace the region of interest with antibiotic selection marker (Table S1). Briefly, the
449 transformation constructs were generated by assembling the amplified flanking regions with the
450 antibiotic resistance cassettes. Between 1-2kb of flanking regions upstream and downstream of
451 the regions of interest were amplified from parental strains using Q5 2x Master Mix (New
452 England Biolabs, USA). The antibiotic resistance gene *ermB* was amplified from *S. pneumoniae*
453 SV35-T23, and the genes, *kan* and *aad9* were amplified from *S. pneumoniae* R6D*ΔbriC::briC*
454 and R6D::spec^{R} (74), respectively. SV35-T23 has an *ermB*-containing mobile element, making it
455 resistant to erythromycin (75). These PCR products were assembled together either by sticky-
456 end ligation of restriction-cut PCR products or by Gibson Assembly using NEBuilder HiFi DNA
457 Assembly Cloning Kit (New England Biolabs, USA).
458
459 The strains *ΔmurMN:murMN* and WT*::alaRS*$_{editing}$ were generated by ligating the gene of interest
460 at its 3' end with an antibiotic resistance cassette. These were assembled with the amplified
461 flanking regions either by sticky-end ligation of restriction-cut PCR products or by Gibson
462 Assembly using NEBuilder HiFi DNA Assembly Cloning Kit. The *murMN* complement strain
463 (*ΔmurMN:murMN*) was recombined at the native *murMN* locus. The WT*::alaRS*$_{editing}$ was
464 introduced downstream of *bga* (without modifying *bga*), a commonly employed site for
465 transformation (74, 76). The *ΔmurMN::alaRS*$_{editing}$ strain was generated by transformation of the

corresponding *alaRS* construct into *ΔmurMN* strain. Primers used to generate the construct are listed in Table S2.

The D39 mutants (D39 *ΔmurMN,* D39 *ΔlytA*, D39*ΔmurMNΔlytA*, D39 *ΔmurMNΔrsh*, D39*ΔmurMN::alaRS*$_{editing}$) were generated by transformation with the corresponding constructs amplified from R6D into strain D39.

Bacterial transformations

To generate mutants, target strains (R6D or D39) were transformed in the following way. Strains were grown in acidic Columbia broth to an OD_{600} of 0.05, followed by the addition of 1µg of DNA along with 125µg/mL of CSP1 (sequence: EMRLSKFFRDFILQRKK; purchased from GenScript, NJ, USA). These treated cultures were incubated at at 37°C for 2 hours. Following the incubation, the cultures were plated on selective Columbia agar plates that contain the appropriate antibiotic: spectinomycin (100µg/ml), erythromycin (2µg/ml), or kanamycin (150µg/ml), and incubated at 37°C overnight. The following day, resistant colonies were selected and cultures in selective media, and colonies were confirmed using PCR. The bacterial strains generated in this study are listed in the Table S1.

Growth curves

Strains of interest were streaked on TSA-II agar plates supplemented with 5% sheep blood (BD BBL, New Jersey, USA). These streaked cells were then inoculated into fresh Columbia broth (normal or acidic) and incubated at 37°C and 5% CO_2 without shaking. Once the cultures reached an OD_{600} of 0.05, the growth of the cultures was followed every 30 minutes by recording their optical density at a wavelength of 600nm.

Strains with a *Δrsh* genetic background showed a much longer lag phase. To circumvent this, when comparing growth of cells with strains in *Δrsh* background, we adapted our protocol from a previous study measuring growth of these cells (37). The cells were grown in acidic Columbia broth to an OD_{600} of ~0.2. The cells were then collected by centrifugation at 3000 rpm for 10 minutes. These cells were then resuspended in acidic Columbia broth to an OD_{600} of approximately 0.1. The growth of these cultures was followed by every 30 minutes by recording their optical density.

All growth curves represented within a given figure panel were carried out in parallel and with the same batch of media.

Cell wall preparation & enzymatic degradation

Pneumococcal cell walls were prepared following a previously published procedure (71). Briefly, after collecting cells by centrifugation, cells were suspended in ice-cold PBS and dropped into boiling sodium dodecyl sulfate to inactivate cell wall-modifying enzymes. The peptidoglycan was further purified using enzymatic degradation as previously described (6).

Analysis of stem peptide composition

The stem peptides contained with the extracted and processed peptidoglycans were separated and analyzed by reverse-phase high-performance liquid chromatography (RP-HPLC) as has been previously described (6).

Thin-layer chromatography (TLC)

S. pneumoniae strains were grown in acidic Columbia broth until an OD_{600} of 0.1 followed by an additional 1-hour incubation. This time-point was chosen so all cells were still in exponential phase, owing to the early lysis observed in *ΔmurMN* cells. The protocol for alarmone labelling

and TLC was adapted from a previous study (37). Cells were harvested by centrifugation at 3300 *g* for 4 minutes. Pellets were washed and the cells were resuspended to the same density in MOPS-CDM. 200µL of the suspension was prewarmed at 37°C for 10 minutes. Following this, 25µL of the warmed suspension was mixed with 150µL of MOPS-CDM containing 150µCi mL^{-1} of $H_3[^{32}P]O_4$ (2mCi mL^{-1} in Water; PerkinElmer, Waltham, MA) for 30 minutes. 25µL of the sample was then removed and mixed with an equal volume of frozen 13M formic acid, followed by repeated thawing and refreezing. After two such cycles, 5µL of the sample was removed for spotting for TLC. The samples were spotted on polyethyleneimine-cellulose (PEI) plastic-baked TLC plates (J.T. Baker) and chromatographed in 1.5M KH_2PO_4 (pH 3.4). TLC plates were then dried, and exposed to a phosphor screen (GE Healthcare, Chicago, IL) overnight. The plates were imaged using Typhoon FLA 9000 imager (GE Healthcare, Chicago, IL) and analyzed using ImageJ.

Antibiotic fitness assay

Pneumococcal cells were grown to mid-exponential phase at an OD_{600} ~0.5 in fresh Columbia broth. Serial dilutions were performed and the cells were plated on either TSA-II blood agar plates or Columbia agar plates with 0.025 µg/ml of penicillin G, and incubated at 37°C and 5% CO_2 overnight. Percent of viable cells was calculated as the ratio of viable CFUs on antibiotic plates relative to viable CFUs on blood agar plates.

Phagocytosis assay

J774A.1 cells (#ATCC® TIB-67™, ATCC, Manassas, Virginia) were grown and maintained in Roswell Park Memorial Institute media (RPMI; Gibco, Gaithersburg, MD) supplemented with 10% fetal bovine serum (Thermo Fisher Scientific, Waltham, MA). J774A.1 cells were certified by IDEXX BioAnalytics (Columbia, MO) to be free of bacterial, fungal or mycoplasma contamination.

542 To test the phagocytosis of wild type and the different pneumococci mutants, 1×10^6 J774A.1 cells
543 were seeded per well in a tissue culture coated 6-well plate (Corning Inc, Corning, NY) and
544 allowed to adhere overnight. Cells were infected in triplicate with 25µl of pneumococcal
545 suspension containing ~3×10^7 CFU resulting in a multiplicity of infection (MOI) of 10 and incubated
546 at 37°C for 1 hour. Post incubation, cells were washed three times with PBS, and incubated for
547 either 30, 60, 120 or 240 minutes in RPMI culture medium containing 10µg/ml penicillin and
548 200µg/ml gentamicin to kill extracellular pneumococci. Cells were then washed five times with
549 PBS and phagocytosed pneumococci were harvested by treating the infected J774A.1 cells with
550 0.025% saponin for 15 minutes at 23 °C. Recovered bacteria were washed in PBS three times
551 and assessed by flow cytometry. For flow cytometry, pneumococci cells were labelled with cell
552 permeant SYTO13 green fluorescent DNA binding dye (Thermo Fisher Scientific, Waltham, MA)
553 according to the manufacturer's instruction prior to infecting J774A.1 cells. Infected J774A.1 cells
554 were manually scrapped, washed and analyzed on Accuri C6 flow cytometer (BD Biosciences,
555 San Jose, CA) connected to an Intellicyt HyperCyt autosampler (IntelliCyt Corp., Albuquerque,
556 NM) using green channel (488 nm). Data were processed and interpreted using FlowJo software
557 (FlowJo LLC, Ashland, Oregon).

558

559 **Confocal microscopy**

560 J774A.1 cells were seeded on 12 mm collagen type-I coated glass coverslips (Electron
561 Microscopy Services, Hatfield, PA) and infected with SYTO13 labeled wild type and the different
562 pneumococci mutants with an MOI of 10 as described above. After 1 hour of infection with labelled
563 pneumococci, J774A.1 cells were washed five times with PBS and treated with 10µg/ml penicillin
564 and 200µg/ml gentamicin for 1 hour to kill extracellular bacteria. Cells were then washed three
565 times with PBS and fixed with 3.33% freshly prepared paraformaldehyde (Electron Microscopy

Services, Hatfield, PA) for 20 min at 23°C. Excess fixative was quenched by adding an equal volume of 1% (w/v) BSA in PBS for 5 min followed by three washes with PBS. To visualize F-actin and nuclei, cells were stained with Alexa Fluor™ 647-Phallodin (Thermo Fisher Scientific, Waltham, MA) (5:200 in PBS) and Hoechst 33342 (Thermo Fisher Scientific, Waltham, MA) (1:1000 in PBS), respectively. Imaging was performed using a Carl Zeiss LSM 880 confocal microscope with fixed settings and the images were analyzed using ZEN Black software (Carl Zeiss Microscopy, Thornwood, NY).

Statistical tests

The statistical differences were calculated using ANOVA. Comparison among different groups was performed using Tukey's post-test. *p* values of less than 0.05 were considered to be statistically significant.

Analysis of the *S. pneumoniae* genomes for AlaXp

A Blastp search was implemented in NCBI. As query we use the AlaXp sequences from Bacillus sp (GenBank WP_000206094.1). Using default parameters, we screened the following NCBI genomes: (1) *Staphylococcus aureus (taxid:1280), Streptococcus thermophilus (taxid:1308), Streptococcus agalactiae (taxid:1311)*, *Streptococcus salivarius (taxid:1304), Enterococcus faecalis (taxid:1351)*, and *Lactobacillus viridescens (taxid:1629)*. All top hits had p-value below 1e-15 and approximately 30% percent identity to the query sequence, except for *Weissella viridescens* and some Enterococci strains that displayed p-value ~1e-9 and percent identity around 25%. Hits were analyzed to establish the starting residue on the query. In all these genomes this number ranged from 489-499, consistent with AlaRS. None of these genomes

589 revealed a hit that matched the AlaXp query in size as well as sequence (although a few partial
590 sequences were identified that appear to correspond to fractions of the AlaRS).
591

592 **ACKNOWLEDGEMENTS**

593 We thank Prof. Alexander Tomasz for introducing us to the study of MurMN through stimulating
594 discussions and challenging questions. We also thank him for providing the R6D strain used in
595 this study. We thank Rory Eutsey and Karina Mueller-Brown for their assistance with laboratory
596 experiments, Manning Huang for help with data visualization, Dr. Aaron Mitchell for productive
597 advice throughout the development of this project, and Dr. John Woolford for a careful reading
598 of this manuscript.
599
600 **FUNDING**

601 This work was supported by NIH grant R00-DC-011322 to NLH, the Stupakoff Scientific
602 Achievement Award to SDA, as well as support from the Eberly Family Trust and the
603 Department of Biological Sciences at Carnegie Mellon University. SF was supported by
604 portuguese national funds from PTDC/BIA-MIC/30746/2017 research grant, from UCIBIO
605 research unit, UID/Multi/04378/2019, and from ONEIDA project (LISBOA-01-0145-FEDER-
606 016417). The funders had no role in study design, data collection and analyses, decision to
607 publish, or preparation of the manuscript.

REFERENCES

1. Silhavy TJ, Kahne D, Walker S (2010) The Bacterial Cell Envelope. *Cold Spring Harbor Perspectives in Biology* 2:a000414.

2. Rajagopal M, Walker S (2017) Envelope Structures of Gram-Positive Bacteria. *Curr Top Micrbiol Immunol* 404:1–44.

3. Koch AL (2003) Bacterial Wall as Target for Attack: Past, Present, and Future Research. *Clinical Microbiology Reviews* 16(4):673–687.

4. Sukhithasri V, Nisha N, Biswas L, Kumar VA, Biswas R (2013) Innate immune recognition of microbial cell wall components and microbial strategies to evade such recognitions. *Microbiological Research* 168:396–406.

5. Tomasz A (1981) Surface Components of Streptococcus pneumoniae. *Reviews of Infectious Diseases* 3(2):190–211.

6. Filipe SR, Tomasz A (2000) Inhibition of the expression of penicillin resistance in Streptococcus pneumoniae by inactivation of cell wall muropeptide branching genes. *Proceedings of the National Academy of Sciences* 97(9):4891–4896.

7. Filipe SR, Severina E, Tomasz A (2001) Functional Analysis of Streptococcus pneumoniae MurM Reveals the Region Responsible for Its Specificity in the Synthesis of Branched Cell Wall Peptides. *The Journal of Biological Chemistry* 276(43):39618–39628.

8. Filipe SR, Pinho MG, Tomasz A (2000) Characterization of the murMN operon involved in the synthesis of branched peptidoglycan peptides in Streptococcus pneumoniae. *The Journal of Biological Chemistry* 275(36):27768–27774.

9. Filipe SR, Severina E, Tomasz A (2000) Distribution of the mosaic structured murM genes among natural populations of Streptococcus pneumoniae. *Journal of Bacteriology* 182(23):6798–6805.

10. Smith AM, Klugman KP (2001) Alterations in MurM, a cell wall muropeptide branching enzyme, increase high-level penicillin and cephalosporin resistance in Streptococcus pneumoniae. *Antimicrobial Agents and Chemotherapy* 45(8):2393–2396.

11. Smith AM, Klugman KP (2000) Non-Penicillin-Binding Protein Mediated High-Level Penicillin and Cephalosporin Resistance in a Hungarian Clone of Streptococcus pneumoniae. *Microbial Drug Resistance* 6(2):105–110.

12. Shepherd J, Ibba M (2013) Lipid II-independent trans editing of mischarged tRNAs by the penicillin resistance factor MurM. *The Journal of Biological Chemistry* 288(36):25915–25923.

13. Shepherd J (2011) Characterisation of Pneumococcal Peptidoglycan Cross-linking Enzymology. PhD Thesis (University of Warwick).

14. Potrykus K, Cashel M (2008) (p)ppGpp: Still Magical? *Annual Review of Microbiology* 62:35–51.

15. Poole K (2012) Bacterial Stress Responses as Determinants of Antimicrobial Resistance. *J Antimicrob Chemother* 67:2067–2089.

16. Hauryliuk V, Atkinson GC, Murakami KS, Tenson T, Gerdes K (2015) Recent functional insights into the role of (p)ppGpp in bacterial physiology. *Nature Reviews Microbiology* 13(5):298–309.

17. Liu K, Bittner AN, Wang JD (2015) Diversity in (p)ppGpp metabolism and effectors. *Current Opinion in Microbiology* 24:72–79.

18. Dalebroux ZD, Svensson SL, Gaynor EC, Swanson MS (2010) ppGpp Conjures Bacterial Virulence. *Microbiology and Molecular Biology Reviews* 74(2):171–199.

19. Dalebroux ZD, Swanson MS (2012) ppGpp: magic beyond RNA polymerase. *Nature Reviews Microbiology* 10:203–212.

20. Maisonneuve E, Gerdes K (2014) Molecular Mechanisms Underlying Bacterial Persisters. *Cell* 157:539–548.

21. Atkinson GC, Tenson T, Hauryliuk V (2011) The RelA/SpoT Homolog (RSH) superfamily: Distribution and functional evolution of ppgpp synthetases and hydrolases across the tree of life. *PLoS ONE* 6(8):e23479.

22. Haseltine WA, Block R (1973) Synthesis of Guanosine Tetra- and Pentaphosphate Requires the Presence of a Codon-Specific, Uncharged Transfer Ribonucleic Acid in the Acceptor Site of Ribosomes. *Proceedings of the National Academy of Sciences* 70(5):1564–1568.

23. Pedersen FS, Lund E, Kjeldgaard NO (1973) Codon specific, tRNA dependent in vitro synthesis of ppGpp and pppGpp. *Nature: New biology* 243(122):13–15.

24. Wendrich TM, Blaha G, Wilson DN, Marahiel MA, Nierhaus KH (2002) Dissection of the mechanism for the stringent factor RelA. *Molecular Cell* 10:779–788.

25. Jenvert R-MK, Schiavone LH (2005) Characterization of the tRNA and ribosome-dependent pppGpp-synthesis by recombinant stringent factor from Escherichia coli. *FEBS Journal* 272:685–695.

26. Filipe SR, Severina E, Tomasz A (2002) The murMN operon: A functional link between antibiotic resistance and antibiotic tolerance in Streptococcus pneumoniae. *Proceedings of the National Academy of Sciences of the United States of America* 99(3):1550–1555.

27. Shepherd J, Ibba M (2014) Relaxed substrate specificity leads to extensive tRNA mischarging by Streptococcus pneumoniae class I and class II aminoacyl-tRNA synthetases. *mBio* 5(5):e01656–14.

28. Tsui WC, Fersht AR (1981) Nucleic Acids Research. *Nucleic Acids Research* 9(18):4627–4637.

29. Schimmel P (2011) Mistranslation and its control by tRNA synthetases. *Philosophical Transactions of the Royal Society B: Biological Sciences* 366(1580):2965–2971.

30. Ahel I, Korencic D, Ibba M, Soll D (2003) Trans-editing of mischarged tRNAs. *Proceedings of the National Academy of Sciences* 100(26):15422–15427.

31. Beebe K, Mock M, Merriman E, Schimmel P (2008) Distinct domains of tRNA synthetase recognize the same base pair. *Nature* 451(7174):90–93.

32. Chong YE, Yang X-L, Schimmel P (2008) Natural homolog of tRNA synthetase editing domain rescues conditional lethality caused by mistranslation. *The Journal of Biological Chemistry* 283(44):30073–30078.

33. Guo M, et al. (2009) Paradox of mistranslation of serine for alanine caused by AlaRS recognition dilemma. *Nature* 462(7274):808–812.

34. Shepherd J, Ibba M (2015) Bacterial transfer RNAs. *FEMS Microbiology Reviews* 39(3):280–300.

35. Guo M, et al. (2009) The C-Ala Domain Brings Together Editing and Aminoacylation Functions on One tRNA. *Science* 325(5941):744–747.

36. Cashel M, Gentry D, Hernandez V, Vinella D (1996) The stringent response. *Escherichia Coli and Salmonella: Cellular and Molecular Biology*, eds Neidhardt F, et al. (ASM Press; Washington, D.C, Washington, D.C), pp 1458–1496.

37. Kazmierczak KM, Wayne KJ, Rechtsteiner A, Winkler ME (2009) Roles of relSpn in stringent response, global regulation and virulence of serotype 2 Streptococcus pneumoniae D39. *Molecular Microbiology* 72(3):590–611.

38. Giudicelli S, Tomasz A (1984) Attachment of pneumococcal autolysin to wall teichoic acids, an essential step in enzymatic wall degradation. *Journal of Bacteriology* 158(3):1188–1190.

39. Gosink KK, Mann ER, Guglielmo C, Tuomanen EI, Masure HR (2000) Role of novel choline binding proteins in virulence of Streptococcus pneumoniae. *Infection and Immunity* 68(10):5690–5695.

40. Maestro B, Sanz J (2016) Choline Binding Proteins from Streptococcus pneumoniae: A Dual Role as Enzybiotics and Targets for the Design of New Antimicrobials. *Antibiotics* 5(2):21.

41. Holtje J-V, Tomasz A (1975) Lipoteichoic acid: a specific inhibitor of autolysin activity in pneumococcus. *Proceedings of the National Academy of Sciences of the United States of America* 72(5):1690–1694.

42. Briese T, Hakenbeck R (1985) Interaction of the pneumococcal amidase with lipoteichoic acid and choline. *European Journal of Biochemistry* 146(2):417–427.

43. Garcia JL, Diaz E, Romero A, Garcia P (1994) Carboxy-terminal deletion analysis of the major pneumococcal autolysin. *Journal of Bacteriology* 176(13):4066–4072.

44. Lardner A (2001) The effects of extracellular pH on immune function. *Journal of Leukocyte Biology* 69:522–530.

719 45. Park S-Y, Kim I-S (2013) Identification of macrophage genes responsive to extracellular
720 acidification. *Inflammation Research* 62(4):399–406.

721 46. Ramos-Sevillano E, et al. (2015) Pleiotropic effects of cell wall amidase LytA on
722 Streptococcus pneumoniae sensitivity to the host immune response. *Infection and*
723 *Immunity* 83(2):591–603.

724 47. Giannouli S, Kyritsis A, Malissovas N, Becker HD, Stathopoulos C (2009) On the role of an
725 unusual tRNAGly isoacceptor in Staphylococcus aureus. *Biochimie* 91(3):344–351.

726 48. Maloney E, et al. (2009) The two-domain LysX protein of Mycobacterium tuberculosis is
727 required for production of lysinylated phosphatidylglycerol and resistance to cationic
728 antimicrobial peptides. *PLoS Pathogens* 5(7):e1000534.

729 49. Raina M, Ibba M (2014) tRNAs as regulators of biological processes. *Frontiers in Genetics*
730 5:171.

731 50. Braeken K, Moris M, Daniels R, Vanderleyden J, Michiels J (2006) New horizons for
732 (p)ppGpp in bacterial and plant physiology. *Trends in Microbiology* 14(1):45–54.

733 51. Wolz C, Geiger T, Goerke C (2010) The synthesis and function of the alarmone (p)ppGpp
734 in firmicutes. *International Journal of Medical Microbiology* 300:142–147.

735 52. Chapeville F, et al. (1962) On the role of soluble ribonucleic acid in coding for amino acids.
736 *Proceedings of the National Academy of Sciences of the United States of America*
737 48(1):1086–1092.

738 53. Prather NE, Murgola EJ, Mims BH (1984) Nucleotide substitution in the amino acid
739 acceptor stem of lysine transfer RNA causes missense suppression. *Journal of Molecular*
740 *Biology* 172(2):177–184.

741 54. Normanly J, Kleina LG, Masson J-M, Abelson J, Miller JH (1990) Construction of
742 Escherichia coli Amber Suppressor tRNA Genes: III. Determination of tRNA Specificity.
743 *Journal of Molecular Biology* 213(4):719–726.

744 55. Tsai F, Curran JF (1998) tRNA2/(Gln) mutants that translate the CGA arginine codon as
745 glutamine in Escherichia coli. *RNA* 4(12):1514–1522.

746 56. Dale T, Uhlenbeck OC (2005) Amino acid specificity in translation. *TRENDS in*
747 *Biochemical Sciences* 30(12):659–665.

748 57. LaRiviere FJ, Wolfson AD, Uhlenbeck OC (2001) Uniform Binding of Aminoacyl-tRNAs to
749 Elongation Factor Tu by Thermodynamic Compensation. *Science* 294(5540):165–168.

750 58. Dale T, Sanderson LE, Uhlenbeck OC (2004) The affinity of elongation factor Tu for an
751 aminoacyl-tRNA is modulated by the esterified amino acid. *Biochemistry* 43(20):6159–
752 6166.

753 59. Asahara H, Uhlenbeck OC (2002) The tRNA Specificity of Thermus thermophilus EF-Tu.
754 *Proceedings of the National Academy of Sciences* 99(6):3499–3504.

755 60. Asahara H, Uhlenbeck OC (2005) Predicting the binding affinities of misacylated tRNAs for
756 Thermus thermophilus EF-Tu·GTP. *Biochemistry* 44(33):11254–11261.

757 61. Li Y, et al. (2015) Identification of pneumococcal colonization determinants in the stringent
758 response pathway facilitated by genomic diversity. *BMC Genomics* 16(1):369.

759 62. Martín-Galiano AJ, et al. (2005) Transcriptional analysis of the acid tolerance response in
760 Streptococcus pneumoniae. *Microbiology* 151(12):3935–3946.

761 63. Piñas GE, Cortes PR, Orio AGA, Echenique J (2008) Acidic stress induces autolysis by a
762 CSP- independent ComE pathway in Streptococcus pneumoniae. *Microbiology*
763 154(5):1300–1308.

764 64. Cortes PR, Piñas GE, Cian MB, Yandar N, Echenique J (2015) Stress-triggered signaling
765 affecting survival or suicide of Streptococcus pneumoniae. *International Journal of Medical*
766 *Microbiology* 305(1):157–169.

767 65. Piñas GE, et al. (2018) *Crosstalk between the serine/threonine kinase StkP and the*
768 *response regulator ComE controls the stress response and intracellular survival of*
769 *Streptococcus pneumoniae* doi:10.1371/journal.ppat.1007118.

770 66. Mellroth P, et al. (2012) LytA, major autolysin of Streptococcus pneumoniae, requires
771 access to nascent peptidoglycan. *The Journal of Biological Chemistry* 287(14):11018–
772 11029.

773 67. Tomasz A, Moreillon P, Pozzi G (1988) Insertional inactivation of the major autolysin gene
774 of Streptococcus pneumoniae. *Journal of Bacteriology* 170(12):5931–5934.

775 68. Sadowy E, Kuch A, Gniadkowski M, Hryniewicz W (2010) Expansion and evolution of the
776 streptococcus pneumoniae Spain 9V-ST156 clonal complex in Poland. *Antimicrobial*
777 *Agents and Chemotherapy* 54(5):1720–1727.

778 69. Cafini F, et al. (2006) Alterations of the penicillin-binding proteins and murM alleles of
779 clinical Streptococcus pneumoniae isolates with high-level resistance to amoxicillin in
780 Spain. *Journal of Antimicrobial Chemotherapy* 57(2):224–229.

781 70. Jensen A, Valdórsson O, Frimodt-Møller N, Hollingshead S, Kilian M (2015) Commensal
782 Streptococci Serve as a Reservoir for β-Lactam Resistance Genes in Streptococcus
783 pneumoniae. *Antimicrobial Agents and Chemotherapy* 59(6):3529–3540.

784 71. Severin A, Tomasz A (1996) Naturally occurring peptidoglycan variants of Streptococcus
785 pneumoniae. *Journal of Bacteriology* 178(1):168–174.

786 72. Paixão L, et al. (2015) Host glycan sugar-specific pathways in streptococcus pneumonia:
787 Galactose as a key sugar in colonisation and infection. *PLoS ONE* 10(3):e0121042.

788 73. Carvalho SM, Kuipers OP, Neves AR (2013) Environmental and Nutritional Factors That
789 Affect Growth and Metabolism of the Pneumococcal Serotype 2 Strain D39 and Its
790 Nonencapsulated Derivative Strain R6. *PLoS ONE* 8(3):e58492.

791 74. Aggarwal SD, et al. (2018) Function of BriC peptide in the pneumococcal competence and
792 virulence portfolio. *PLOS Pathogens* 14(10):e1007328.

793 75. Hiller NL, et al. (2011) Differences in Genotype and Virulence among Four Multidrug-
794 Resistant Streptococcus pneumoniae Isolates Belonging to the PMEN1 Clone. *PLoS ONE*
795 6(12):e28850.

796 76. Zähner D, Hakenbeck R (2000) The Streptococcus pneumoniae beta-galactosidase is a
797 surface protein. *Journal of Bacteriology* 182(20):5919–5921.

798

FIGURE LEGENDS

Fig. 1. Growth defects observed in the absence of *murMN*. (A) Representative growth curves for wild-type and Δ*murMN* strains grown in normal (●) and acidic conditions (▲). Growth curves were started at an OD_{600} of 0.05 *(at least n=3)*. **(B)** Representative growth curves for wild-type, Δ*murMN* and Δ*murMN:murMN* strains grown in acidic conditions (▲). Growth curves were started at an OD_{600} of 0.05 *(at least n=3)*. **(C)** Box-and-whisker plot depicting median and range of maximum growth of wild-type, Δ*murMN* and Δ*murMN:murMN* strains grown in acidic conditions. 'ns' denotes non-significant comparison and **** $p<0.0001$ relative to wild-type strain by ANOVA followed by Tukey's post-test.

Fig. 2. Analysis of peptidoglycan structure of cells grown in normal and acidic conditions. HPLC profiles of the stem peptide compositions of peptidoglycan from **(A.i)** wild-type and **(A.ii)** Δ*murMN* strains grown in normal and acidic pH. **(B)** Structures of the cell wall stem peptides that comprise pneumococcal peptidoglycans.

Fig. 3. Analysis of translation quality control function of MurM (A) Schematic representation of the domain architecture of full-length and ectopically expressed editing domains of AlaRS. **(B)** Different tRNA moieties that can be deacylated by MurM (underlined). *In blue*: Mischarged tRNA moieties that can be edited by $AlaRS_{editing}$ protein. *In green:* All other mischarged tRNA moieties that can be edited by MurM but not $AlaRS_{editing.}$ Schematic based on findings from previous work (12, 27). **(C)** Representative growth curve for wild-type, Δ*murMN* and *ΔmurMN::alaRS*$_{editing}$ strains grown in acidic conditions (▲). Growth curves were started at an OD_{600} of 0.05 *(at least n=3).*

Fig. 4. MurMN regulates stringent response pathway. (A) Schematic of (p)ppGpp production and hydrolysis. **(B)** Thin-liquid chromatography showing ^{32}P being incorporated as GTP or alarmones (ppGpp or pppGpp) in wild-type, Δ*murMN* and Δ*murMN*Δ*rsh* strains grown in acidic conditions. Ratio of alarmone to GTP in Δ*murMN* is 3.7-fold times that in the wild-type. **(C)** Representative growth curve for wild-type, Δ*murMN*, Δ*rsh* and Δ*murMN*Δ*rsh* strains grown in acidic conditions (▲). To circumvent the long lag phase of strains from Δ*rsh* background, strains were grown to log phase (~OD_{600} 0.2), collected by centrifugation and growth curves started at an OD_{600} of 0.1 *(at least n=3)*.

Fig. 5. LytA-mediated autolysis is triggered in Δ*murMN* cells. (A) Representative growth curve for wild-type and Δ*murMN* strains grown in acidic conditions (▲), either in the absence or presence of 2% choline chloride. Growth curves were started at an OD_{600} of 0.05. **(B)** Representative growth curve for wild-type, Δ*murMN, ΔlytA* and Δ*murMNΔlytA* strains grown in acidic conditions (▲). Growth curves were started at an OD_{600} of 0.05. *(at least n=3)* **(C)** Schematic representing change in the distribution of LytA (triangles). When strains are growing in exponential phase, LytA is localized mainly intracellularly (*left*) but when they reach stationary phase, LytA is exported to the surface resulting in autolysis (*right*), based on findings from Mellroth *et al.* (66).

Fig. 6. MurMN controls LytA-mediated evasion from phagocytosis. Internalization of pneumococcal cells with J774A.1 macrophages. **(A)** Confocal microscopy images depicting bacterial internalization after 60mins. *In blue*: macrophage nuclei, *red:* bacterial cells, *green*: actin. **(B)** Quantification of J774A.1 macrophages positive for pneumococci after 30mins, as separated by flow cytometry. 'ns' denotes non-significant comparisons, *** $p<0.001$, and **** $p<0.0001$ relative to wild-type; ^^^^ $p<0.0001$ relative to Δ*murMN*, by ANOVA followed by Tukey's post-test. Graph also shows expected LytA activity for each strain, '+' denotes basal levels, '++' denotes increased levels and '-' denotes absence.

Figure 1

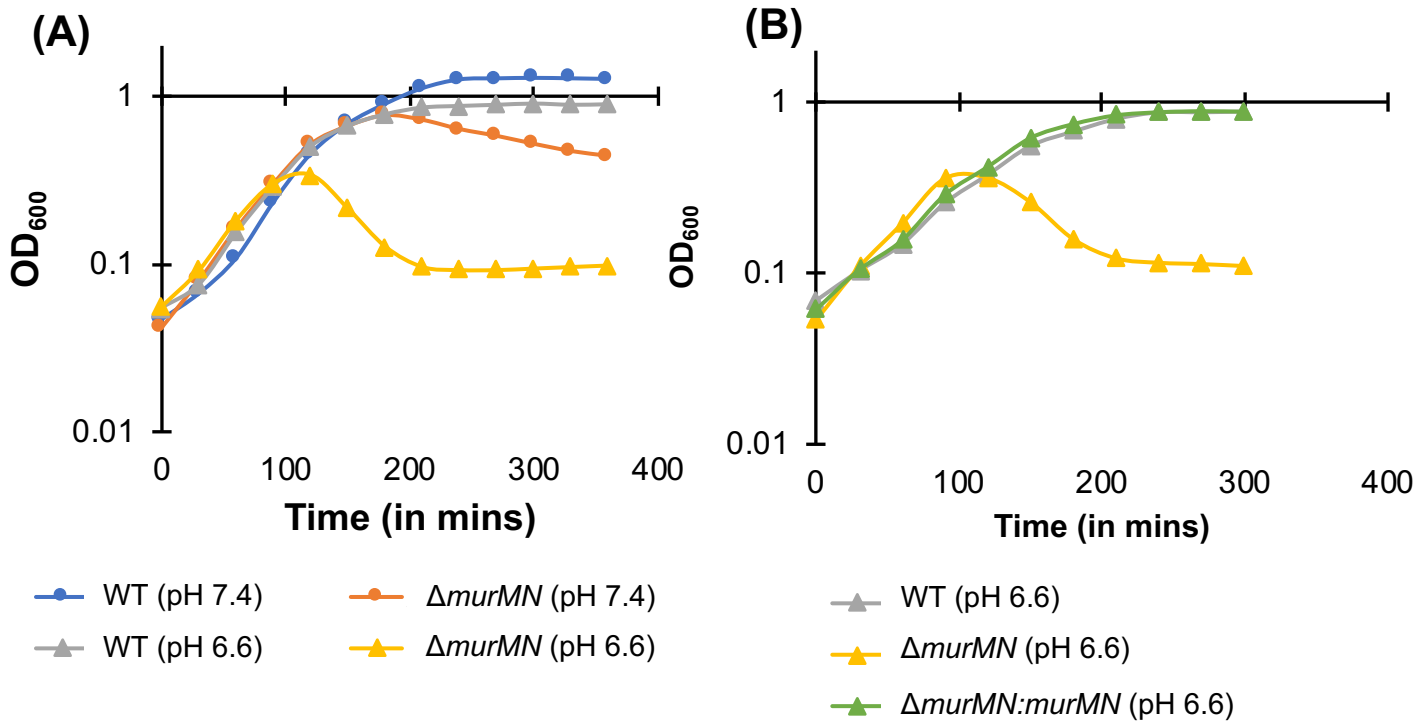

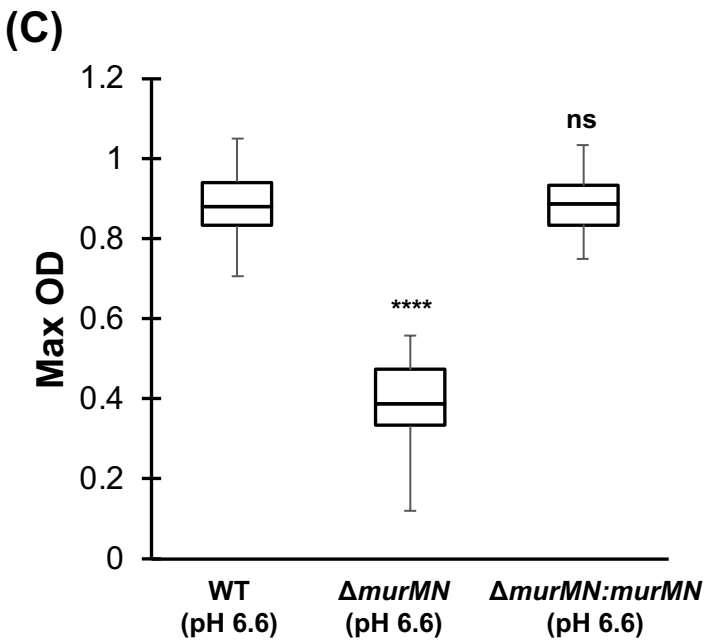

Figure 2

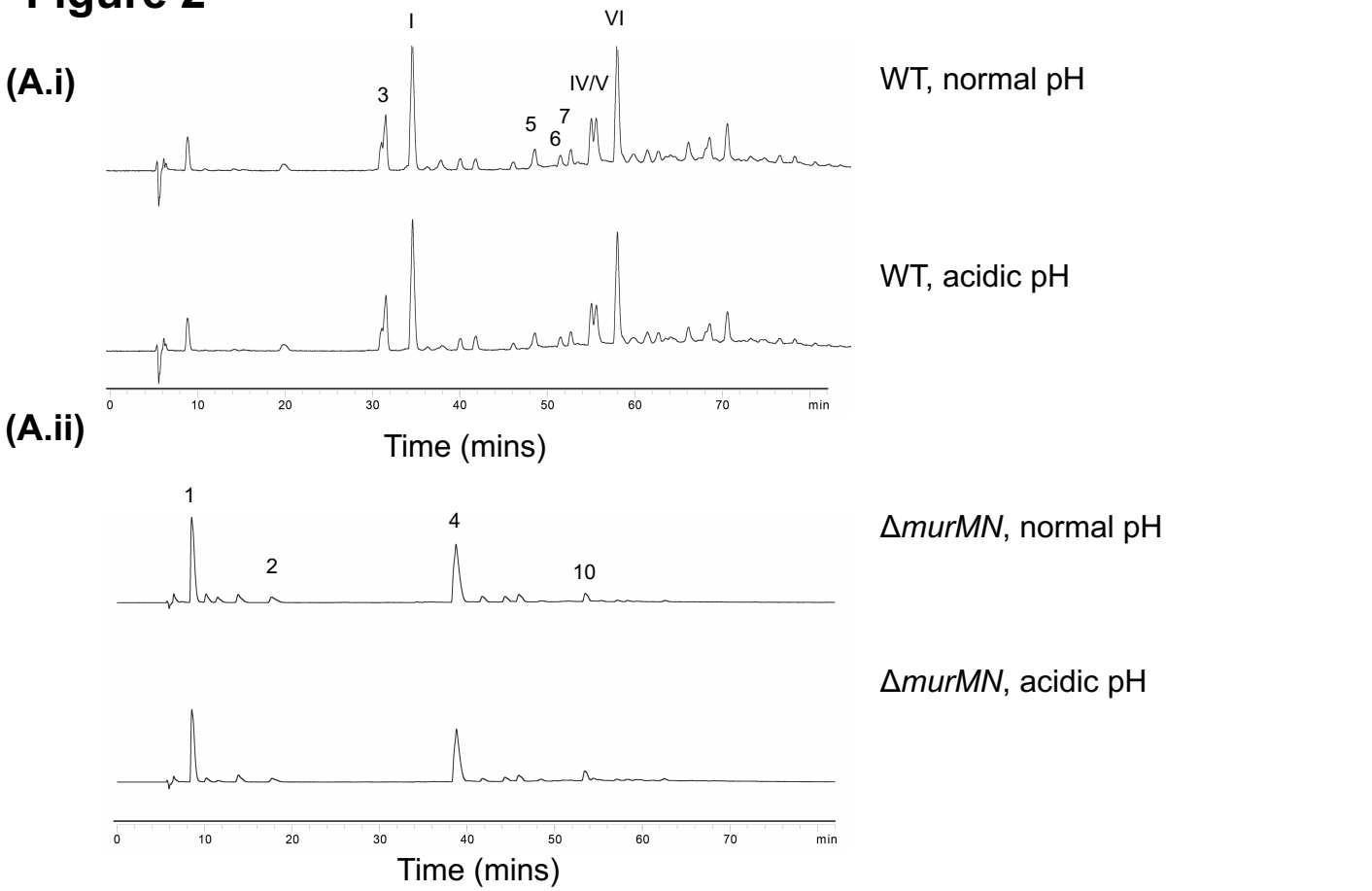

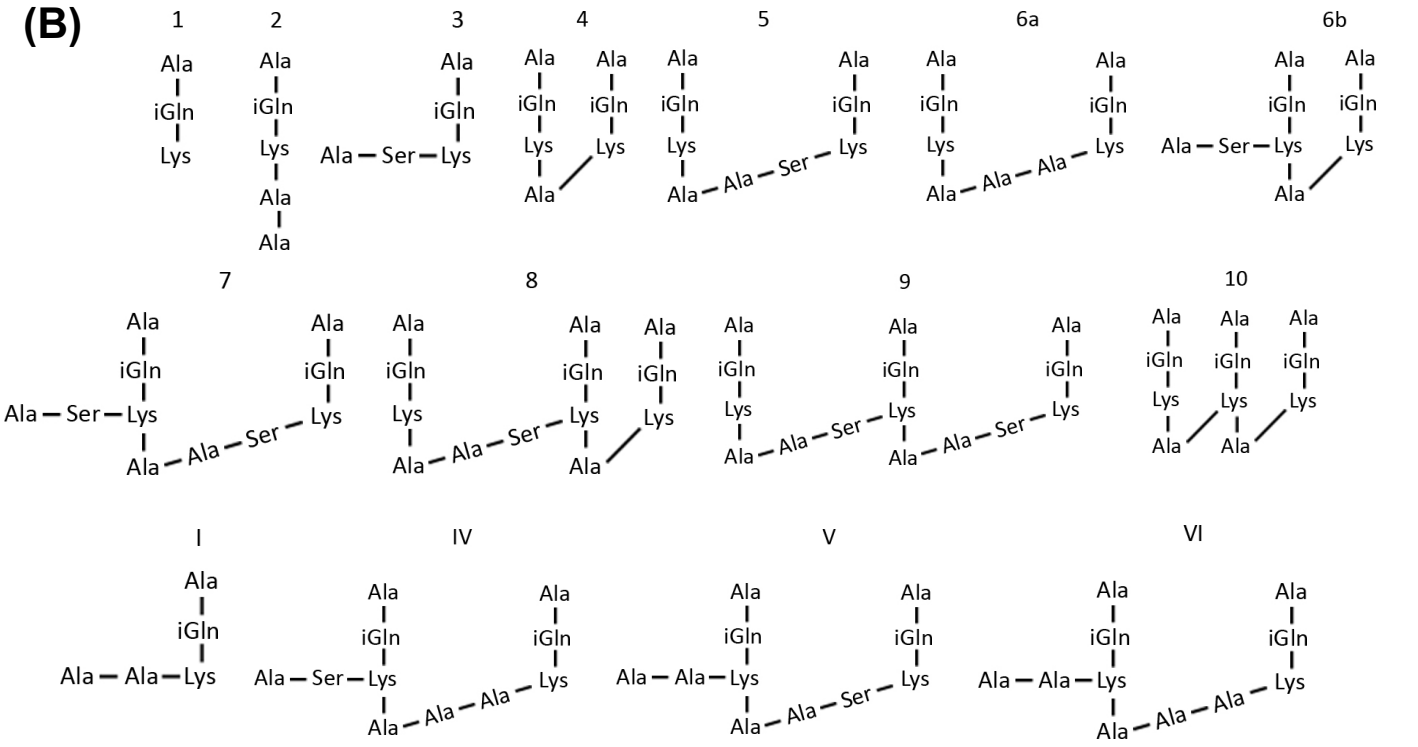

Figure 3

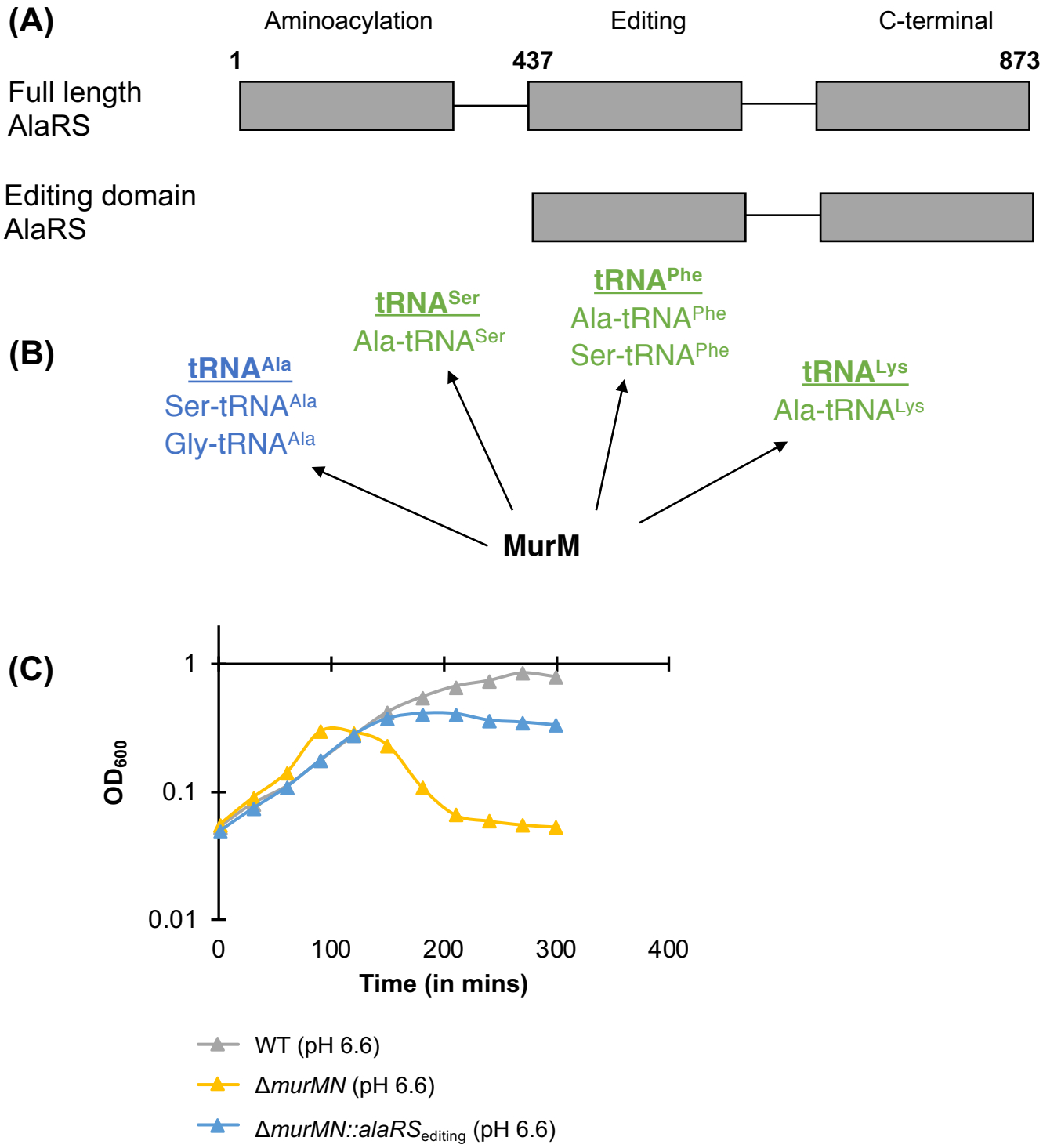

Figure 4

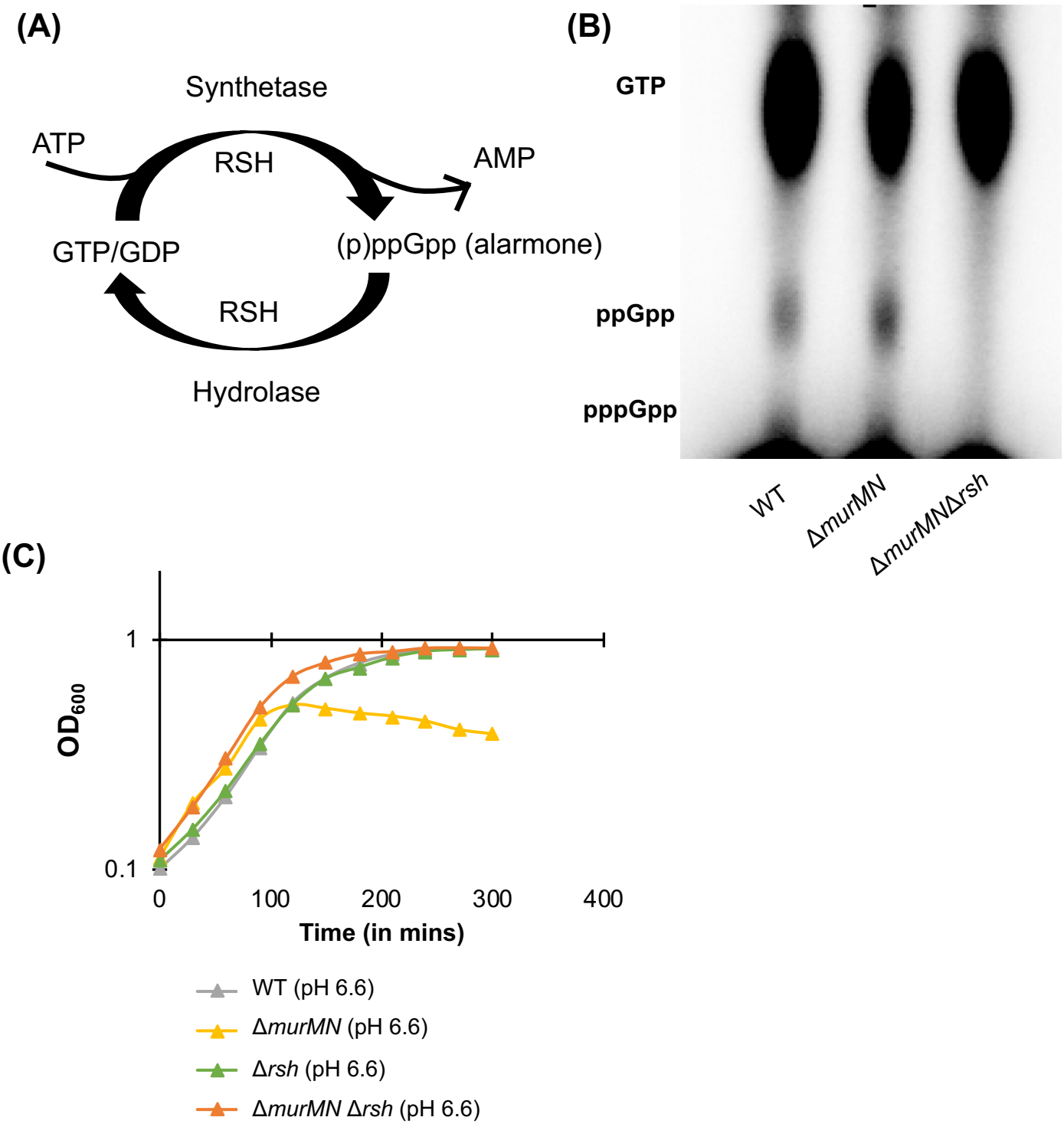

Figure 5

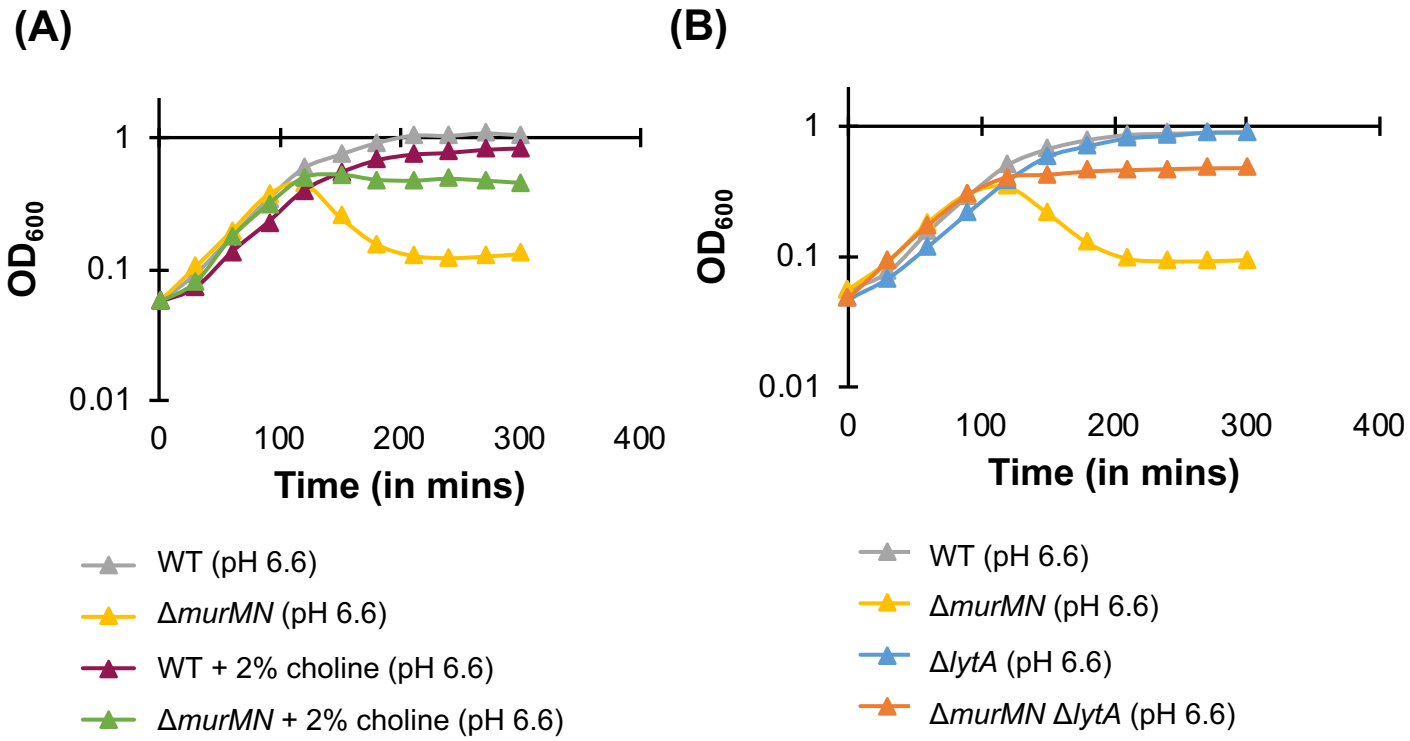
(A)
1
0.1
0.01
OD600
0
100
200
300
400
Time (in mins)
WT (pH 6.6)
ΔmurMN (pH 6.6)
WT + 2% choline (pH 6.6)
ΔmurMN + 2% choline (pH 6.6)
(B)
1
0.1
0.01
OD600
0
100
200
300
400
Time (in mins)
WT (pH 6.6)
ΔmurMN (pH 6.6)
ΔlytA (pH 6.6)
ΔmurMN ΔlytA (pH 6.6)

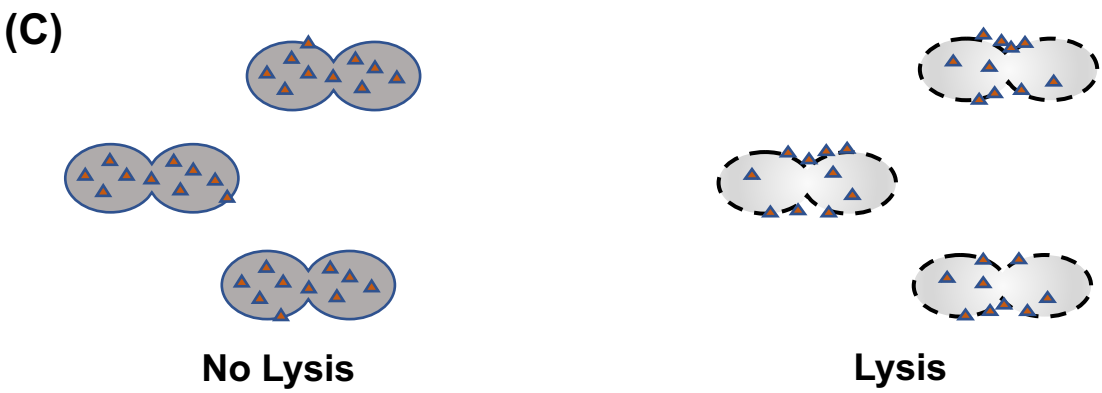
(C)
No Lysis
Lysis

Figure 6

(A)

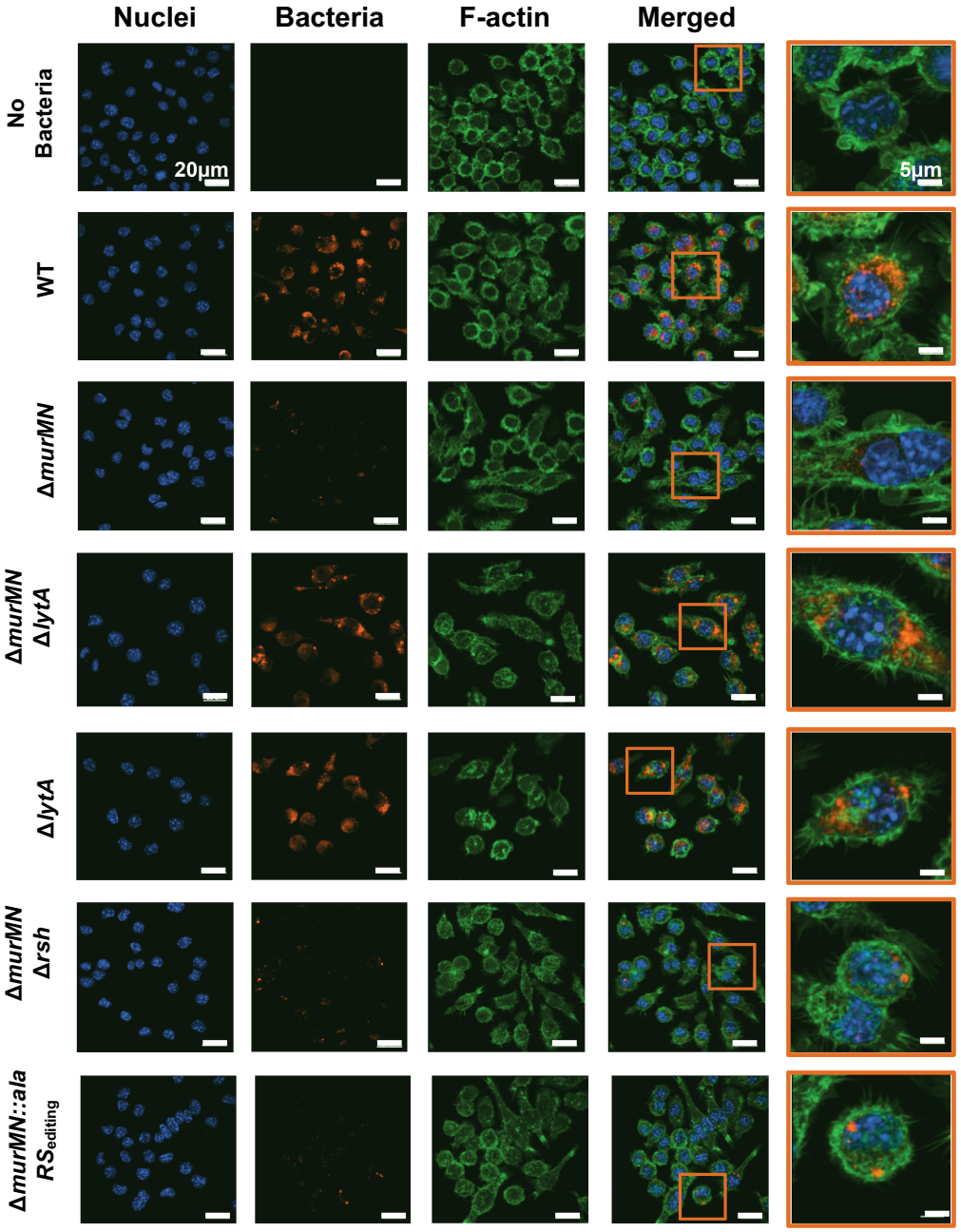
Nuclei
Bacteria
F-actin
Merged
No Bacteria
WT
ΔmurMN
ΔmurMN ΔlytA
ΔlytA
ΔmurMN Δrsh
ΔmurMN::ala RSediting
20μm
5μm

(B)

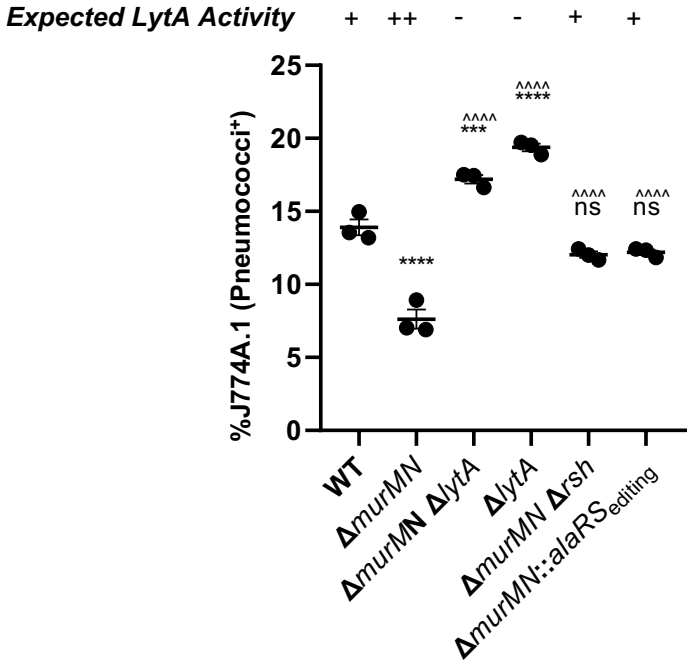
Expected LytA Activity
+ ++ - - + +
%J774A.1 (Pneumococci+)
25
20
15
10
5
0
****
^^^^ ***
^^^^ ****
^^^^ ns
^^^^ ns
WT
ΔmurMN
ΔmurMN ΔlytA
ΔlytA
ΔmurMN Δrsh
ΔmurMN::alaRSediting

Table 1: Percentage Viable CFUs of Different Strains after Growth in Penicillin G. Table represents percentage viability from three independent biological replicates.

	Penicillin 0.025 µg/ml		
Strain	**Replicate 1**	**Replicate 2**	**Replicate 3**
Δ*murMN*	0	0	0
Δ*murMN::alaRS* $_{editing}$	16	40	30
Δ*murMN* Δ*rsh*	5	10	53
WT	68	89	94
WT*::alaRS* $_{editing}$	98	72	83
Δ*rsh*	44	123	76